European Geothermal Congress 2013
Pisa, Italy, 3-7 June 2013

Geothermal potential of a sedimentary reservoir in Northern Germany - deduced from stochastic modelling

Christian Vogt[1], Katja Iwanowski-Strahser[2], Wolfgang Rabbel[2], Gabriele Marquart[1] and the MeProRisk Research Consortium

[1] Institute for Applied Geophysics and Geothermal Energy, E.ON Energy Research Center, RWTH Aachen University, Mathieustr. 10, 52074 Aachen, Germany

[2] Institute of Geosciences, Christian-Albrecht-University of Kiel, Otto-Hahn-Platz 1, 24118 Kiel, Germany

cvogt@eonerc.rwth-aachen.de

Keywords: Reservoir modelling, Monte Carlo, probability of success, exploration risk.

ABSTRACT

We investigate the probability for a successful geothermal heat production installation in a sedimentary reservoir in the Northern German Lowland. The stratigraphy and the target layer are identified in a 3D seismic section of 5 km x 5 km lateral length down to 6 km. We establish histograms for the lithological properties based on logging information and measurements on cutting from a number of drill holes. These histograms are interpreted as probability distributions for the rock properties in a stochastic sense. We use numerical modelling to study the transient flow and temperature variations in a Monte Carlo ensemble of 1 000 realisations where rock properties are assigned according to these histograms using Sequential Gaussian Simulation. We study a single and a double well geothermal installation in the target layer and determine the probability of success based on a projected flow rate of 42 L s^{-1} and a temperature of 75 °C; this installation is supposed to supply 4000 local households with heat. Even though it turns out that for this particular location the combined probability of success is only 1.6 %, this study demonstrate the capability of stochastic modelling to infer the potential of a reservoir for geothermal use.

1. INTRODUCTION

Accurate prognosis of flow rate and temperature as well as quantifying the corresponding uncertainties are crucial factors when planning a geothermal installation such as a doublet. Stochastic numerical modelling allows for addressing these factors.

In this paper, we present a case study in a depleted oil and gas reservoir in the northeastern German sedimentary basin. It is potentially interesting for geothermal development and was studied regarding geothermal energy use by Hahne et al. (2011).

The target region is located in the center of the basin where the temperature field is not affected by the several salt domes within this region. Using 3D inversion of temperature data obtained in the wells, Vogt et al. (2013) estimated a specific heat flow of (77.7 ± 1.2) mW m^{-2} at 6 km depth. This is in good agreement with the results of a study of Norden et al. (2008) who found an average geothermal temperature gradient of about 35 K km^{-1} for this region.

Based on the results obtained by a regional model from Vogt et al. (2013) (see also paper entitled "MeProRisk-II – a joint research project for optimization strategies and risk analysis for deep geothermal reservoirs" in this conference), we focus here on estimating transient pressure and temperature variations as well as the corresponding uncertainties during the operation of a geothermal doublet within a detailed reservoir model of the target layer, the Upper Triassic Rhaetian sandstone at a depth of about 2 km. There, the initial temperature is (87.1 ± 1.8) °C (Vogt et al. 2013).

We assume minimum requirements for flow rate and temperature of 42 Ls^{-1} and 75 °C, respectively. This would allow warm-water support of 4000 households as projected e.g. in The Hague, The Netherlands (Mottaghy 2011). Consequently, the Rhaetian sandstone at a depth range of 1928 m – 1951 m is selected as target horizon for five reasons: (i) it is characterized by an increased porosity of about 10 %; (ii) at least sparse permeability data are available from hydrocarbon exploration, (iii) the steady-state temperature prediction satisfies the minimum requirement of 75 °C, (iv) an empirical relationship between porosity and permeability is available for this horizon (Pape et al. 2005); (v) the target horizon is enclosed by impermeable layers of clay-rich rocks.

As an alternative, we study a single and a double well layout making use of one out of several large tectonic faults within the layers deposited from the Middle Triassic to the Lower Jurassic.

Cherubini et al. (2011) modeled the influence of faults in this region on the temperature field. Tischner et al. (2010) discussed a single-well concept for deep geothermal systems as an alternative to double-well systems. They tested two concepts: (i) a huff-puff scheme where water is first injected in and then produced from the same target layer, and (ii) circulation between two horizons connected by a stimulated hydraulic fracture. In the present study, we test also a single-well concept with circulation in two layers connected by a natural fault.

2. GEOTHERMAL INSTALLATION IN A SEDIMENTARY LAYER

The geometry of the reservoir is derived from a 3D seismic data set (Figure 1(a)) and from a stratigraphic model (Figure 1(b)) constructed using Petrel (Schlumberger 2012) based on about 100 boreholes down to a depth of 2500 m plus one borehole (Z-1) with a depth of 6000 m.

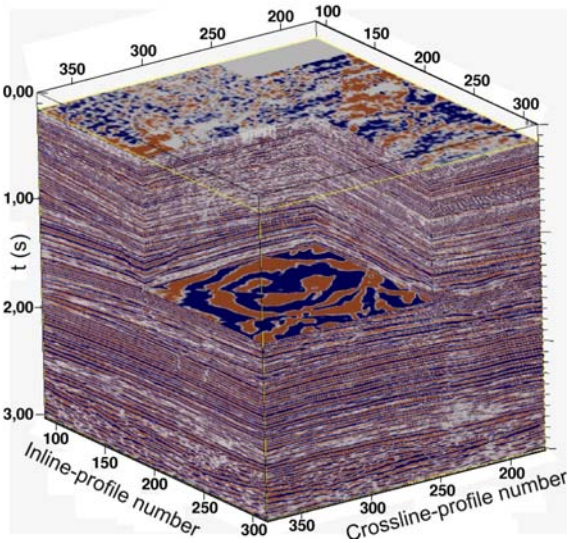

(a)

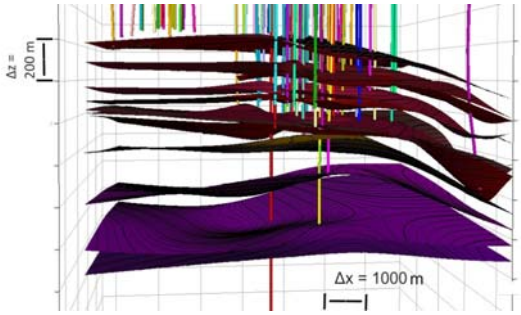

(b)

Figure 1: Data sets used to derive a geometric reservoir model (Vogt et al. 2013): (a) reflection amplitude polarities (red and blue) in a 3D seismic data cube (128 inline profiles × 202 crossline profiles × time t), and (b) stratigraphic model produced with the Petrel software (Schlumberger, 2012) from about 100 boreholes.

The 3D reflection seismic data set, provided by RWE Dea AG, images sediments in the northeastern German basin in a cube of a horizontal area of about 5 km × 5 km and a depth of 6 km. The seismic data set consists of 128 inline profiles × 202 crossline profiles. In Figure 1(a), the seismic amplitudes are sign-color-coded and plotted versus recording time. For inferring depth, the seismic velocity model is calibrated based on sonic logs from wells and mean velocities from geophone measurements. With the help of borehole information and logging data from one deep borehole, the depth column is divided into 18 major units and groups of layers. The interfaces between the layers are afterwards identified in the 3D seismic data. Since the thickness of some of the layers is below seismic resolution, data from the deep borehole Z-1 is essential to calibrate the depths of the picked horizons. This concerns also the target horizon. Finally, the locations of the layers inside the geometrical model are verified by comparison with information from the stratigraphic model at all borehole positions (Figure 1(b)).

To test the usefulness of this reservoir for a geothermal installation we perform simulations of hydrothermal flow in a porous medium using the software SHEMAT-Suite (Rath et al. 2006).

We assume a hypothetical doublet within the target layer with a borehole distance of 500 m and simulate the operation in a detailed reservoir model (1000 m × 1500 m × 225 m) with grid cells of 20 m × 20 m × 5 m. According to seismic interpretation, the region comprises no major faults. The inclined target horizon is vertically discretized with at least three grid cells. The caprock layers directly above and below the target layer are included also in the model. We assign constant temperatures taken from the regional thermal model of Vogt et al. (2013) to the top (84.5 °C) and base (93.0 °C) of the model. Since the target horizon extends laterally beyond the model boundaries, we fix the initial hydraulic head constant at the model boundaries. This allows fluid in- and outflow across the boundaries. However, numerical tests show that the model is laterally large enough to suffer only little from the influence of the hydraulic boundary conditions. We implement a circulation rate of 42 L s^{-1} and a re-injection temperature of 40 °C. 900 numerical time steps for 20 years of simulation time prove to be sufficient for all realizations, because an increased number of time steps do not yield different temperature predictions.

2.1 Hydraulic Rock Properties

A stochastic approach is applied for generating 400 Monte Carlo realizations of the spatial porosity distribution and, hence, for addressing its heterogeneity and uncertainty. These realizations are equally-likely to reflect reality defined by a porosity distribution inverted from logging data taken from the Z-1 well. The realizations are generated using Sequential Gaussian Simulation (Deutsch and Journel 1998).

Permeability is the primary rock property controlling fluid flow. Unfortunately, no permeability data are available from any borehole within the target region. Therefore, we use an empirical relationship between porosity φ and permeability k, available for the Rhaetian sandstone (Pape et al. 2005):

$$k = 0.309(100\varphi)^{4.85} \times 10^{-18}\ (\mathrm{m}^2). \qquad [1]$$

Sparse permeability data from adjacent regions and from the same lithology (personal communication by RWE Dea AG) confirm the relationship within the given errors (Figure 2). In the following, we use the original parameters of Pape et al. (2005) in equation [1].

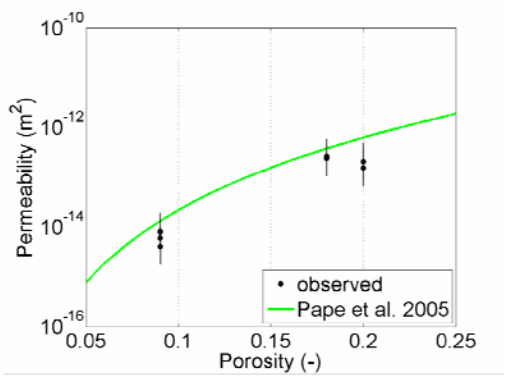

Figure 2: Observed permeability in the Rhaetian sandstone (personal communication by RWE Dea AG) and empirical porosity-permeability relationship of Pape et al. (2005).

Figure 3 illustrates the observed porosity and calculated permeability histograms used to create stochastic spatial porosity and permeability variations for the modelling.

Based on these rock properties and the given boundary conditions, we simulate heat transport and fluid flow for each single realization using the simulator SHEMAT-Suite for a period of 20 years.

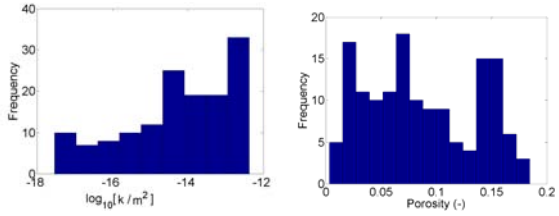

(a) (b)

Figure 3: (a) Observed histrogram of porosity in the Rhaetian sandstone and (b) corresponding permeability *k* calculated following Pape et al. (2005).

2.2 Results

Figure 4 shows reservoir temperature for one sample of the 400 Monte Carlo realizations after 20 years of heat production together with the corresponding porosity and permeability field. However, in Monte Carlo modelling, one single realization contains little information. Therefore, we focus on the entire ensemble of realizations to provide results.

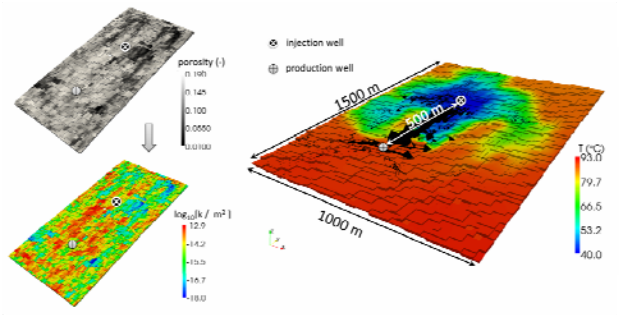

Figure 4: Reservoir porosity, corresponding permeability after Pape et al. (2005), and corresponding temperature for one Monte Carlo realization after 20 a of heat production. Velocity arrows indicate the flow direction. The two dots indicate the injection and production point of the doublet. Heterogeneity in temperature result from heterogeneities in permeability, not from boundary effects.

We evaluate the number of ensemble realizations meeting the requirements for pressure and temperature for estimating the success probability of a hypothetical geothermal project. By using a Monte Carlo ensemble, we obtain a best estimate (ensemble mean) of the temperature and its uncertainty (ensemble standard deviation) after 20 years of operation.

As the fulfillment of temperature requirement is easily obtained from the simulation result, the flow rate $q_w = vA$ is implemented as a boundary condition, where A is the well surface and v the Darcy velocity. To evaluate whether this flow rate can be really established, we make the following consideration:

v depends on reservoir pressure drop. Given a certain flow rate, insufficient permeability k may result in pressure drops which are not achievable by common pumps. Therefore, pressure is also of major importance for evaluating the risk of the geothermal project. This pressure can be evaluated stochastically from the Monte Carlo ensemble of realizations. To this end, we calculate the pressure inside the well p_w for each realization from the corresponding simulated block pressure p_b of the grid cell in the numerical model which represents the production well. We follow the semi-analytical approach of Peaceman (1983) for the case of fluid production:

$$p_w = p_b - q_w\mu_f / (2\pi k\Delta z)\ \ln(r/r_w). \qquad [2]$$

Here, the flow rate q_w is 0.042 $m^3\ s^{-1}$, Δz the vertical cell size is 5 m, r_w the well radius is 0.08 m, and r is the equivalent radius of the cell, defined for cubic cells of size Δx and isotropic permeability by:

$$r = 0.14\ \mathrm{sqrt}(2\Delta x) \qquad [3]$$

with $\Delta x = 20$ m in this case.

In some realization, production pressure decreases with time as a result of the predefined constant flow rate in combination with too low permeability close to the well allowing no sustainable recharge. Thus, the well pressure may become negative after some years according to equation [3]. Of course, in a real-world reservoir, negative absolute pressure cannot be realized. In this case, we interpret that the given circulation rate of 0.042 m^3 s^{-1} cannot be sustained.

Now, we can evaluate the probability of success of the installation from the ensemble after 20 years of operation (Figure 5). We identify all realizations featuring a temperature above 75 °C and non-negative pressure at the required flow rate of 42 L s^{-1} as successful and promising for operating the reservoir. We determine how many realizations meet the requirements for temperature (16.3 %), for pressure (22.8 %) and both combined (1.6 %). In general, we find an early thermal breakthrough, i.e. an arrival of cold water at the production borehole, after only a few years. A larger borehole distance would result in a later thermal breakthrough. However, a larger distance corresponds to a larger pressure drop at the production borehole. Due to the very low probability of success (1.6 %) for the hypothetical project, we recommend not to use the Rhaetian sandstone in this area as a reservoir for a geothermal doublet within the defined requirements.

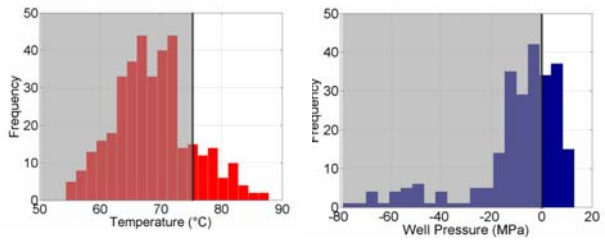

(a) (b)

Figure 5: (a) Temperature and (b) pressure distribution according to the stochastic ensemble after 20 years of operation. Also shown are the projected requirements for a geothermal installation (vertical lines). For the temperature requirement (a) the threshold is supposed to be similar to the heat-use project in The Hague, The Netherlands (Mottaghy et al., 2011). For well pressure (b), negative values indicate that the flow rate requirement of the heat-use project cannot be reached.

3. INSTALLATION USING IDENTIFIED FAULTS

During seismic interpretation, different fractures and faults were detected within the regional model. Due to the predicted insufficient performance for the target sandstone, we study an alternative design using a fluid circulation along one of these detected fault zone connecting the two sandstone aquifers middle Rhaetian sandstone and Angulate sandstone. The latter is located about 150 m above the Rhaetian sandstone.

For modelling fracture-bound fluid flow, detailed information is needed on the structure of faults, in particular the targeted one. Complex fracture networks offer potential pathways for fluids or may act as barriers. Detailed knowledge as well as an assessment of its reliability is essential. To detect these fractures, we apply an automatic fracture detection algorithm which can handle the large amount of data. The algorithm is based on the fact that sediments mostly feature plain coherent reflectors in which fractures manifest themselves as lateral disturbances. Therefore they can be detected using a coherence-based algorithm described by Gersztenkorn & Marfurt (1999). After a dip calculation based on the gradient structure tensor (Bakker, 2002), an analysis cube (small sub-volume of the data set) containing parameters describing the seismic signal is moved along the reflecting horizons. At the same time, the data covariance matrix $\boldsymbol{C}$ is assembled for each analysis cube. After computing i positive eigenvalues λ_i of $\boldsymbol{C}$, a measure for the coherence level E is than given by:

$$E = \lambda_1 / \Sigma \lambda_i, \qquad [4]$$

with $0 \leq E \leq = 1$. Each analysis cube is described by one value E. Large values of E indicate large coherence. Therefore, fault displacement in the horizons is identified by lateral minima of E. Thus, for each sub-volume, we obtain the information whether it is part of a fracture structure or not.

The fracture inventory of the study location is classified into two domains: an upper zone with a great amount of small cracks and a lower zone, near the target horizon, which is dominated by larger fractures.

As an additional verification, we checked the size-frequency distribution of the automatically detected faults that turn out to be compatible with fractal distributions typically found for geologically mapped fault systems (Turcotte 1997).

3.1 Numerical Model

Figure 6 show the model which includes the two sandstone layers and a fault. The model comprises 101 x 101 x 51 grid cells. The boundaries are isolating for fluid flow and heat transport.

For all models, we assume again a circulation rate of 42 L s^{-1} and a homogeneous permeability of 10^{-13} m^2 for the target layers. Initial hydraulic heads and temperatures are taken from the regional temperature model (Vogt et al. 2013). Re-injection temperature is 40 °C.

Geometrically the fault zone is modelled by a minimum of three cells of dimension 5 m × 5 m × 5 m. As the real lateral extension of the fault zone is unknown, we assume these dimensions to avoid disturbance of the modelled fault zone by an insufficiently fine discretization.

Again, the simulation extends over 20 years, discretized into 15 000 numerical time steps of equal length of about 12 hours. We study different permeabilities (10^{-14} m^2 – 10^{-11} m^2) and porosities (5 % – 20 %) for the fault zone.

Potential mechanical or chemical effects (such as permeability or porosity changes) due to the re-injection of reservoir brine into a different horizon are ignored.

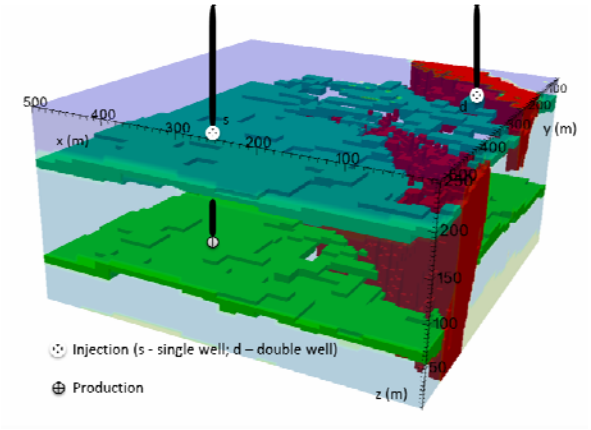

Figure 6: Fault layout for a single geothermal well with injection point at (s) and geothermal doublet with injection at point (d). Angulate sandstone (dark green) and middle Rhaetian sandstone (light green) and fault zones (red) are shown, dense layers in between are hidden. Permeabilities are assumed as homogeneous within each sandstone layer (10^{-13} m^2) and the fault zones (10^{-14} m^2 – 10^{-11} m^2).

3.2 Single Well Layout

In a first scenario (s) is based on just one geothermal well. We assume thermally isolated fluid flow within the geothermal well for upstream and downstream (a best-case assumption). This allows the injection of cold water in the upper (Angulate) sandstone, circulation through the fault zone and the production of warm water from the lower (Rhaetian) sandstone using just one well.

This scenario has the additional advantage of requiring only one well for operation. Since drilling costs are a major part of the project cost, saving one borehole may make a project more attractive for investors.

Since we have no data for estimating the hydraulic characteristics of the fault zone, we cannot quantify, as previously, the uncertainty of reservoir performance in a Monte Carlo scheme. In contrast, we use a simplified approach based on different possible connectivity cases. To this end we study the sensitivity of pressure and temperature variation with time on different average fault zone permeabilities and porosities. We simulate two different scenarios regarding the distance between well and fault zone: (i) ~250 m and (ii) ~40 m. Figure 6(s) illustrates the well position near the fault zone in scenario (i).

The results of these simulations for scenario (i) are shown in Figure 7 for (a) temperature and (b) well pressure, respectively, assuming various permeabilities and porosities for the fault zone. Obviously, also in this single well scenario, an early thermal breakthrough occurs after about 2.5 years of operation time. All hydraulic scenarios show a similar temperature variation with time. Surprisingly, a high permeability of 10^{-11} m^2 results in higher temperatures after 20 years of operation. This might be explained in the following way: The steeper drop at the beginning due to a good hydraulic connectivity is offset because hot water from deeper parts of the fault is produced at later operation time resulting in somewhat warmer production fluid at later times. For $k = 10^{-14}$ m^2, the simulation is numerically unstable due to the low resulting pressure. A production scenario would fail, as for k = 10^{-13} m^2 and k = 10^{-12} m^2 because well pressure drops below zero. This indicates that the circulation rate cannot be sustained after about 7 years and 15 years, respectively, as discussed above. Only the best-case scenario with a permeability of 10^{-11} m^2 and a porosity of 20 % maintains a sufficient well pressure for continuous heat production. However, for a real installation, the well needs to be placed further away from the fault or the distance between the chosen targeted sandstone layers should be larger to avoid an early thermal breakthrough.

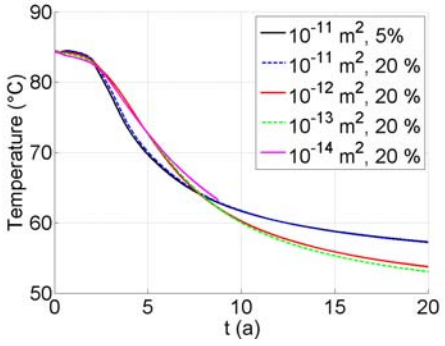

(a)

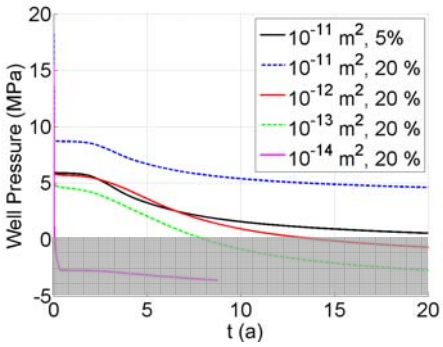

(b)

Figure 7: Transient variation of (a) temperature and (b) well pressure for different hydraulic properties (permeability and porosity of the fault zone) for scenario (i) at the production level of the single well layout.

Figures 8 compares the results for scenario (ii) where the well is closer to the fault zone in comparison with the best result for scenario (i) with a permeability of 10^{-11} m^2. In scenario (ii), the length of the direct flow paths is shorter by about 445 m. In terms of pressure, this scenario is more suitable. A similar pressure is obtained even though permeability is one order of magnitude lower. However, due to the short distance the thermal breakthrough occurs much earlier. The temperature declines to 60 °C already before five years of operation. Thus, a geothermal installation is not feasible under the given requirements, but could well be operated if lower temperatures are satisfying for direct heat use. To make use of a fault for a geothermal reservoir in geologic conditions similar to the studied ones, we therefore recommend a distance of at least 250 m between well and fault.

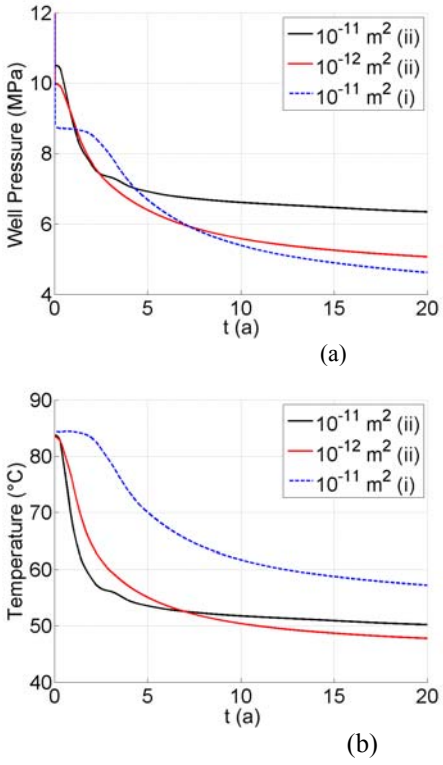

Figure 8: Transient variation of (a) temperature and (b) well pressure for different hydraulic properties (permeability and porosity of the fault zone) for scenarios (i) and (ii) at the production level of the single well layout. Porosity is 20 % in all cases.

3.3 Double Well Layout

All scenarios so far are characterised by an early thermal breakthrough, making the feasibility of a geothermal installation questionable. In order to avoid this, we study another doublet scenario making use of different faults connected by permeable layers. This way, the subsurface heat exchanger surface is increased. The production well is identical to the one in the single well layout in scenario (i), but the injection well is placed as visualised in Figure 6(d). Circulation rate and temperature as well as simulation time as chosen as before. For the fault, we assume best-case conditions of a permeability of 10^{-11} m^2 and a porosity of 20 %.

Figure 9 shows the result of this approach in comparison to the single well approach of scenario (i). Making use of the fault network maintains higher production temperatures as estimated. However, the hydraulic connection of the fault-layer-network seems to be insufficient, resulting in negative pressures after few years. Again, this indicates that the circulation rate cannot be established.

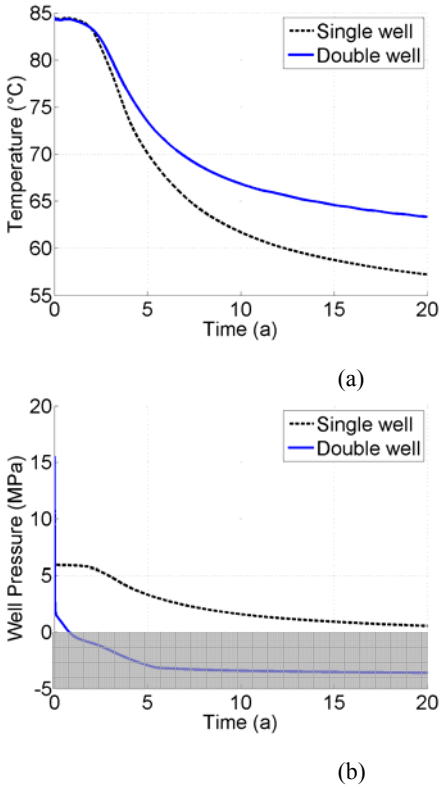

Figure 9: Transient variation of (a) temperature and (b) well pressure for a double well layout making use of the fault network.

Figure 10 illustrates the velocity field as well as the temperature inside the fault system and inside the Rhaetian sandstone layer (target horizon). Unfortunately, the cold water front does spread only in the secondary fault where water is injected; and takes a direct path through the main fault, not cooling this structure before reaching the production well. This leads to an early thermal breakthrough.

3. CONCLUSIONS

We studied different layouts for hypothetical geothermal installations in a reservoir in the north-eastern German sedimentary basin. To this end, we used log and laboratory data from wells in the target region, stochastic numerical modelling, and a given porosity-permeability relationship.

For both, single well or doublet scenarios, the small thickness of the target sandstones combined with insufficient permeabilities does not support a successful heat production. For a doublet in a sedimentary layer, the probability of success is only 1.6 %. Even a larger distance between the wells for avoiding the early thermal breakthrough is unlikely to help, because of the expected larger pressure drop resulting from a larger distance.

To overcome this obstacle, an alternative approach is conceivable. It may comprise, besides hydraulic or chemical stimulation, making use of existing faults in the region for single or double well concepts. Such faults were identified by seismic interpretation based on a minimum-coherence algorithm. According to our findings, a fault permeability of 10^{-11} m^2 and a porosity of 20 % or more are most suitable for operation in terms of variation of pressure and temperature with time. For the single well concept, suitable well pressures due to high permeabilities do not prevent high temperatures, because hot water may be produced from deeper regions of the fault. However, the distance between the target layers in a real installation should be significantly larger than the one in this study (40 m – 200 m) as long as the pressure drop, i.e. the permeability distribution, allows this. We recommend a distance of at least 250 m between well and fault. In addition, an isolated piping in the well may be required when using a one-well design to avoid cooling of the produced water within the well.

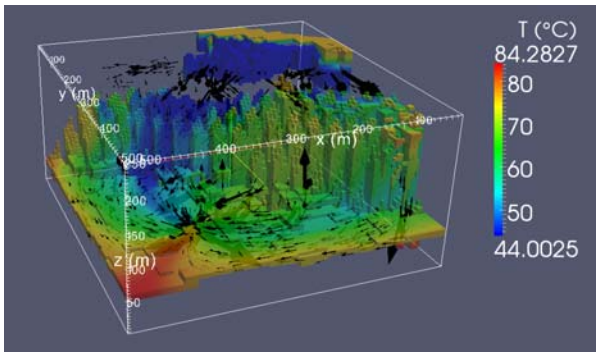

Figure 10: Temperature inside the fault system and inside the Rhaetian sandstone layer (target horizon) indicated by colour as well as filtration velocity indicated by the arrows after 20 years of production.

Circulation in a network of faults interconnected by sedimentary layers in a doublet layout did not yield sufficient connectivity in this case. Therefore, the single well concept proved to be preferable here.

When interpreting results, it must be mentioned that we did not account for chemical reactions within the reservoir. A temperature drop due to cold water injection may also change the reservoir's chemical equilibrium, resulting in chemical precipitation or dissolution. The latter may clog the pore space, resulting in an increase of permeability. This effect may alter the flow regime significantly. However, this will require additional numerical simulation of chemical reactions similar to the implementation by Clauser (2003).

An additional approximation is the neglect of any stress field, which could yield information on whether faults are more likely to be open or sealed for fluid flow. Further changes of pressure due to forced circulation may affect the permeability, in particular fault permeability. Accounting for this will require the simulation of geomechanics, e. g. following the approach of Watanabe et al. (2010).

However, simulating different geothermal installations in their geological setting allows quantifying their chance of success.

REFERENCES

Bakker P.: Image structure analysis for seismic interpretation, Doctoral dissertation, *Delft University of Technology*, (2002).

Cherubini Y., Cacace M. and Scheck-Wenderoth M.: Assessment of the impact of faults on the coupled fluid and heat transport in a geothermal site (Groß Schönebeck, NE-German Basin): first results from 3d finite element simulations, *Geophysical Research Abstracts*, **13**, (2011), EGU2011-2514.

Clauser C., editor: Numerical simulation of reactive flow in hot aquifers, SHEMAT and processing SHEMAT, *Springer*, Heidelberg-Berlin, (2003).

Deutsch, C. and Journel, A.: GSLIB. Geostatistical software library and user's guide, *University Press*, Oxford (1998).

Gersztenkorn A. and Marfurt K.: Eigenstructure-based coherence computations as an aid to 3-D structural and stratigraphic mapping, *Geophysics*, **64**, (1999), 146814-79.

Hahne B., Thomas R. and the gebo Geosystem Team: Combined geoscientific investigations of geothermal reservoir characteristics in Lower Saxony, Germany, *Geophysical Research Abstracts*, **13**, (2011), EGU2011-10054

Mottaghy D., Pechnig R., Taugs R., Kröger J., Thomsen C., Hese F. et al.: , et al.: Geothermal 3-D modeling Hamburg and surrounding areas: temperature prediction and reservoir simulation, *Geophysical Research Abstracts*, **13**, (2011), EGU2011-8684-1.

Norden B., Förster A. and Balling N.: Heat flow and lithospheric thermal regime in the Northeast German Basin, *Tectonophysics*, **460**, (2008), 215-229.

Pape H., Clauser C., Iffland J., Krug R. and Wagner R.: Anhydrite cementation and compaction in geothermal reservoirs: interaction of pore-space structure with flow, transport, p-t-conditions, and chemical reactions. *International Journal of Rock*

Mechanics and Mining Sciences, **42**, (2005), 1056-1069.

Peaceman D.: Interpretation of well-block pressure in numerical reservoir simulation with non-square grid blocks and anisotropic permeability, *Society of Petroleum Engineers Journal*, **23**, (1983), 531-543.

Rath V., Wolf A. and Bücker M.: Joint three-dimensional inversion of coupled groundwater flow and heat transfer based on automatic differentiation: sensitivity calculation, verification, and synthetic examples, *Geophysical Journal International*, **167**, (2006), 453-466

Schlumberger: Petrel, (2012), http://www.slb.com/services/software/geo/petrel.aspx [retrieved: 18.03.13].

Tischner T., Evers E., Hauswirth H., Jatho R., Kosinowski M. and Sulzbacher H: New concepts for extracting geothermal energy from one well: the GeneSysproject, *Proceedings of the 2010 World Geothermal Congress*, Bali, Indonesia, (2010), paper #0464.

Turcotte D.: Fractals and chaos in geology and geophysics, U*niversity Press*, Cambridge, (1997).

Vogt C., Iwanowski-Strahser K., Marquart G., Arnold J., Mottaghy D., Pechnig R., Gnjezda D. and Clauser C.: Modeling contribution to risk assessment of thermal production power for geothermal reservoirs, *Renewable Energy*, **53**, (2013), 230-241.

Watanabe N., Wang W., McDermott C., Taniguchi T., Kolditz O.: Uncertainty analysis of thermo-hydro-mechanical (THM) coupled processes in heterogeneous porous media, *Computational Mechanics*, **45**, (2010), 263-280.

Acknowledgements

This project was funded by the German Federal Ministry for Education and Research (BMBF) under grant 03SF0326A.We thank the MeProRisk team for fruitful discussion and RWE Dea AG, Hamburg, for kindly providing proprietor reservoir data.